The Surface of Ordered Mesoporous Benzene−Silica Hybrid Material: An Infrared and ab Initio Molecular Modeling Study

Barbara Onida,[†] Luisa Borello,[†] Claudia Busco,[‡] Piero Ugliengo,[‡] Yasutomo Goto,[§] Shinji Inagaki,[§] and Edoardo Garrone*[,†]

Dipartimento di Scienza dei Materiali e Ingegneria Chimica, Politecnico di Torino, Corso Duca degli Abruzzi, 24, 10138 Torino, Italy, Dipartimento di Chimica IFM, Università di Torino, Via P. Giuria, 7, 10125 Torino, Italy, and Toyota Central R&D Laboratories, Inc., Nagakute, Aichi, 480-1192, Japan

Received: February 8, 2005

Joint IR and computational results allow a detailed characterization of the surface properties of a mesoporous benzene−silica hybrid material with crystal-like wall structure. After outgassing at 450 °C, hydroxyl species mainly consist of noninteracting silanols, with both O−H and Si−O stretching modes at lower frequencies than those of SiOH in silica. Interaction with several probe molecules, followed both by experiment and calculus, shows that the aryl group in the coordination sphere of Si imparts a lesser acidity with respect to the isolated silanol in silica. In contrast, adsorption isotherms indicate that the interaction with acetone is stronger with benzene−silica than with silica: this is interpreted in terms of secondary interactions taking place between the slightly acidic CH in acetone and the electronic cloud in benzene-like rings. This suggests that both the inorganic component and the organic one play a role in dictating the surface behavior.

Introduction

Aromatic-silica materials with periodic mesoporous structure have been recently synthesized[1−6] from organosilane precursors and surfactant templates. These PMO systems (periodic mesoporous organosilica) are hybrid materials capable of further processing, imparting properties as functional materials, adsorbents, and catalysts, for example, aromatic groups may allow anchoring of active functionalities such as sulfonic groups.[7]

In 2002, Inagaki and co-workers reported the first preparation of a mesoporous benzene−silica hybrid material with highly ordered walls, so as to suggest a nearly crystalline structure. On the basis of X-ray diffraction and NMR evidence,[8] the idealized model in Figure 1 has been proposed, showing hydrophilic and hydrophobic parallel rows of silica and benzene, respectively. Silanols pave the internal surface as it would occur in ideal ordered mesoporous silica. The magnification of the idealized structure (section b) shows the presence of pairs of stacked benzene rings, about 4.4 Å far apart, and of isolated silanols, all equivalent, involving a Si atom linked to two oxygen atoms and one carbon atom of a benzene ring. The presence of such silanols is documented by ^{29}Si NMR spectroscopy.[8]

The potential properties of this ordered surface are fascinating: for instance, periodicity could have a role in orienting guest species, with implications as it concerns catalytic or optoelectronic applications. The present paper reports a study of its adsorptive properties by means of joint FTIR spectroscopy and ab initio molecular modeling. Because of the hybrid nature of the solid, natural reference systems are, on one hand, the isolated silanol of amorphous silica and, on the other hand, the benzene molecule.

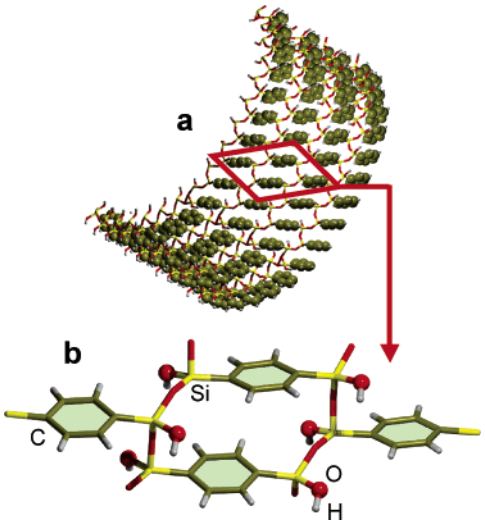

Figure 1. (a) Cartoon of a portion of the wall of benzene−silica: benzene rings are shown as hexagons of C atoms, represented by van der Waals spheres. (b) Magnification of a significant portion, showing in particular silanol groups and the occurrence of pairs of stacked benzene hexagons.

Experimental Section

FTIR Study. The ordered mesoporous benzene−silica hybrid material has been prepared and characterized as in ref 8. For FTIR measurements, the powder has been pressed into thin self-supporting wafers, which have been placed into a quartz cell, allowing thermal treatments in controlled atmosphere. Before adsorption, the sample has been outgassed at 723 K. Spectra have been recorded using a Bruker FTIR Equinox 55 spectrometer, equipped with an MCT cryodetector, at a resolution of 2 cm^{-1}. Dosage of gases and vapors has been carried out by connecting the IR cell to a vacuum frame (residual pressure $<10^{-3}$ mbar). CO and N_2 adsorption was studied at low temperature (nominal 77 K), whereas all other molecules have

* Corresponding author. E-mail: edoardo.garrone@polito.it.
† Politecnico di Torino.
‡ Università di Torino.
§ Toyota Central R&D Laboratories, Inc.

10.1021/jp050686n CCC: $30.25
Published on Web 05/27/2005

been adsorbed at room temperature. Gases were from Messer; liquids for vapor adsorption were analytical grade reagents from Sigma-Aldrich.

Ab Initio Calculations. Ab initio calculations on molecular models have been carried out using GAUSSIAN98 program.[9] The nonlocal hybrid B3LYP[10] density functional has been used as level of theory coupled with the standard 6-31+G(d,p) basis set, which ensures a good compromise between chemical accuracy and cost of the calculations.[11]

The binding energies (BE) of the intermolecular complexes considered have been computed by subtracting the energies of the separate molecular constituents from the total energy of the complex. No correction for the basis set superposition error (BSSE) has been made for two reasons. On one hand, the computations being contrasted with experimental data of spectroscopic nature, the interest in binding energies is less cogent. On the other hand, as it concerns BE, we carry out only comparisons between the interaction of the same basic probe with closely similar acidic partners, for which BSSE is expected to be the same; previous experience with B3LYP/6-31+G(d,p) suggests that it will amount to about 25% of the total BE value.[12]

On the optimized structures, the whole set of vibrational frequencies have been computed in the harmonic approximation. Anharmonic correction to the OH stretching frequency has been evaluated for the free models by computing the OH fundamental frequency as follows: (i) the O−H distance has been assumed as a pure normal mode, decoupled with respect to all other modes; (ii) the O−H distance was varied around its equilibrium value (−0.2/+0.3 Å, with 0.02 Å step) and the total energy was computed at each distance; and (iii) a sixth-degree polynomial curve has been used to fit the points (root-mean-square error less than 10^{-6} Hartree), and the 1D nuclear Schroedinger equation has been solved following the algorithm proposed by Lindberg[13] and coded in the program ANHARM.[14] Stretching frequencies calculated in the harmonic approximation are designated as ω_h, those coming from the anharmonic treatment as ω_{01}, and the experimental ones as ν.

Manipulation and visualization of structures have been dealt with the MOLDRAW program,[15,16] and the POVRAY program using input files prepared by MOLDRAW has rendered molecular drawings.

Results and Discussion

Vibrational Properties of the Naked Sample. The three sections of Figure 2 report the FTIR spectrum of benzene−silica outgassed at 723 K in the range 3800−600 cm^{-1}. Basically, section a shows the stretching modes of silanols and C−H species, section b reports several peaks due to aromatic rings modes, and section c shows the bending modes of SiOH species together with the stretching modes of structural Si−O groups. A minor feature in section a is the tailing in the region 3700−3500 cm^{-1} discussed below. The inset to Figure 2a compares the IR spectrum in the O−H stretching region of benzene−silica and of an amorphous mesoporous all-silica sample pretreated at the same temperature.

Isolated Silanols. The OH and Si−OH stretching modes, ν(OH) and ν(Si−OH), are, respectively, at 3730 cm^{-1} (Figure 2a, arrow) and 926 cm^{-1} (Figure 2c, arrow). Both values are lower than the corresponding values for silanols in amorphous silica[17] (3747 and 960 cm^{-1}, Table 1), respectively, by 17 cm^{-1} (stretching) and 34 cm^{-1} (bending).

In the field of siliceous systems, a lower value of Si−OH stretching frequency is often connected to a more pronounced acidic character of the proton. As no literature data are available concerning isolated molecules with phenyl−Si−OH groups, to understand if this is the case, an ad-hoc molecular modeling has been carried out. First, a molecular cluster model has been assumed for silanols in the hybrid material, and the results of computations have been compared with the experimental vibrational features of the Si−OH species. At a later stage, the interaction of SiOH species with several probe molecules has been studied, both from the experimental and computational points of view.

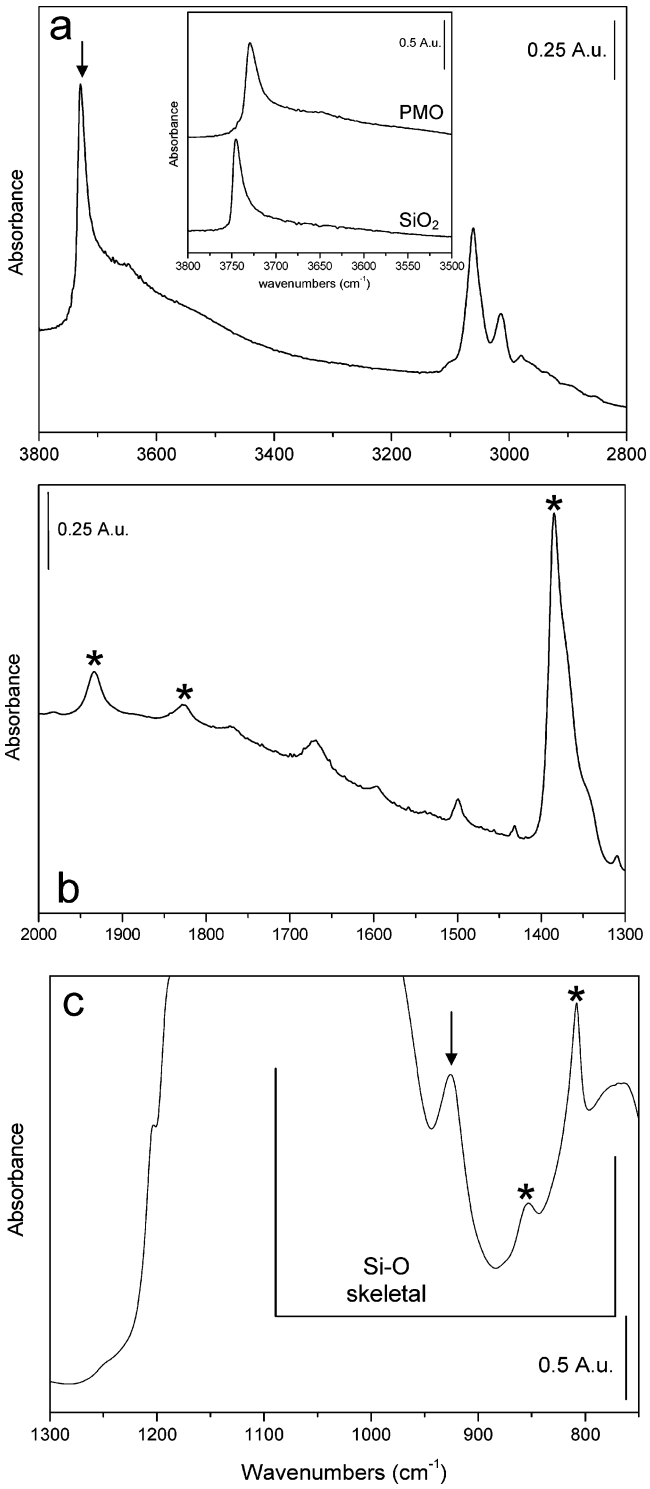

Figure 2. IR spectra of benzene−silica outgassed at 723 K in different spectral ranges. The inset compares the OH stretching mode of benzene−silica (PMO) with that of mesoporous silica.

TABLE 1: B3LYP/6-31+G(d,p) Harmonic ω_h(OH), Anharmonic ω_{01}(OH) Stretching, and ν(Si−OH) Stretching Frequencies of SIL and SILH Models[a]

model	ω_h(OH)	ω_{01}(OH)	ν(OH) (expt)	ν(Si−OH)	ν(Si−OH) (expt)
SIL	3902	3741	3747	926	960
SILH	3893	3731	3730	912	926
Δ(SIL−SILH)	9	10	17	14	34

[a] Experimental values are for amorphous silica and for benzene−silica, respectively. Δ is the difference between SIL and SILH values. All data in cm^{-1}.

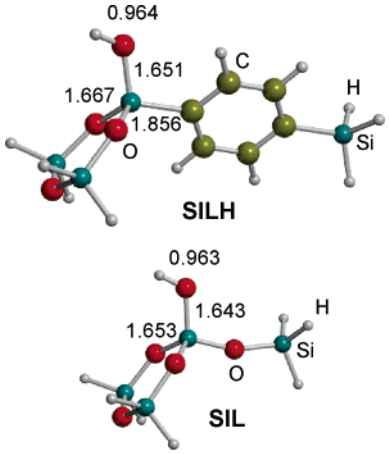

Figure 3. B3LYP/6-31+G(d,p) optimized structures of SIL and SILH as models for the isolated silanols of amorphous silica and benzene−silica, respectively. Bond length in Å.

The cluster model assumed is depicted in Figure 3. This is referred to as SILH, standing for silanol in the hybrid system. The cluster model is large enough to ensure that the OH stretching frequency is well reproduced[18] but still affordable in terms of computational power, if account is taken that targets of computations are not only the energy-minimum structures but also the more demanding harmonic and anharmonic frequencies, the former to be computed also for the clusters interacting with the probe molecules. The basic ingredients of the model are the silanol group, a phenyl group in its first coordination sphere, together with two oxygen atoms. These are part of a six-membered SiO ring linked to the SiOH moiety ensuring the structural rigidity needed to avoid artifacts during geometry optimization. SILH does not correspond to a fragment of the structure in Figure 1 terminated by H atoms. To keep as much structural similarity as possible with the SILH model, a cluster model for the isolated silanol in amorphous silica has also been assumed (referred to as SIL, Figure 3). Both structural similarity and rigidity ensure that the differences between the OH vibrational frequency of SILH and SIL clusters are due to electronic effects rather than to different local geometrical strain around the SiOH group.

Calculated values of the OH and Si−OH stretching frequencies for SIL and SILH are reported in Table 1. In agreement with the experiment in passing from SIL to SILH, a decrease of both stretching modes is computed, indicating that differences in vibrational features have to be ascribed to electronic effects due to neighboring atoms. Inclusion of anharmonicity effects brings calculated and experimental values remarkably close to one another.

Other OH Stretching Bands. A broad tailing in the range 3700−3200 is seen (Figure 2a) because of H-bonded silanols, probably occurring at defects in the pore walls, as no pair of silanols interacting via H-bond are present in the idealized structure of Figure 1.

TABLE 2: Comparison between Selected Infrared Modes of Benzene−Silica, as Compared to Those of Benzene and SILH[a]

assignment	benzene (B3LYP)	benzene (expt)[b]	SILH (B3LYP)	benzene−silica (expt)
ν_4	712	703	767	808
ν_{10}	863	849	875	853
$\nu_{10}+\nu_{17}$	1846	1815	1873	1826
$\nu_5+\nu_{17}$	1996	1955	1986	1936
ν_{19}	1514	1480	1412	1384

[a] Assignments follow the standard notation for the benzene modes. Data in cm^{-1}. [b] See ref 22.

The weak signal occurring at 3645 cm^{-1} (which has no counterpart in siliceous systems) is probably due to traces of aromatic C−OH species,[19] formed by the cleavage of Si−C bonds. Such cleavage has been observed by means of ^{29}Si CP-MAS NMR by Ozin and co-workers for a similar system treated at the same temperature in nitrogen:[20] it is ascribed to the nucleophilic attack of silicon atoms of Si−C (benzene) by atmospheric water or by Si−OH groups, a process common in PMOs during thermolysis.[21]

Aromatic Rings. The assignment of most of the observed IR modes related to the organic component in benzene−silica has been done by comparing the experiment in Figure 2 with computational results for SILH as well as for the benzene molecule. CH stretching modes (section a) give rise to a triplet of bands because of the occurrence of a Fermi resonance. The components fall, however, at lower frequencies in benzene−silica than in the benzene molecule. This has been already observed with sol−gel derived phenyl silicates[23] and is obtained here through the ab initio computations.

As to ring vibrations, Table 2 reports a selection of experimental modes (both fundamental vibrations and combinations, labeled by asterisks in the Figure), for which an assignment is proposed. The approach adopted is based on the observation of which modes (ν_{11}, $\nu_5+\nu_{17}$, ν_5, ν_{19}) decrease in frequency when passing from benzene to SILH, whereas ν_{10}, ν_4, and $\nu_{10}+\nu_{17}$ behave the opposite.[22]

Interaction with Probe Molecules. To compare the acidic properties of the silanol in benzene−silica with that of the isolated silanol of amorphous silica, recourse has been made to the classical procedure of measuring the bathochromic shift in O−H stretching mode imparted by the same probe molecule to the two acidic species. When a set of molecules is employed, the plot of one set of shifts, concerning one acidic species, against the set concerning the other species leads to a straight line (the so-called Bellamy−William−Hallam plot), the slope of which is a measure of the relative acidity of the two species.[24]

Figure 4 illustrates the set of spectra obtained by contacting the benzene−silica with eight basic molecules able to interact with the Si−OH moiety through H-bonds. These vary in basic strength from the very weak nitrogen molecule to proper bases such as ammonia. A shift of the Si−OH stretch is seen from the initial value of 3730 cm^{-1}, the extent of which depends on the proton affinity of the molecule.[25] Relevant data are reported in Table 3; also reported in the table are the corresponding literature data concerning the SiOH group in amorphous silica. Table 3 shows that values in this latter set are invariably larger than the corresponding ones in the former set, that is, the Si−OH group in the hybrid material is less acidic than that in amorphous silica; accordingly, the BWH plot in Figure 5 shows

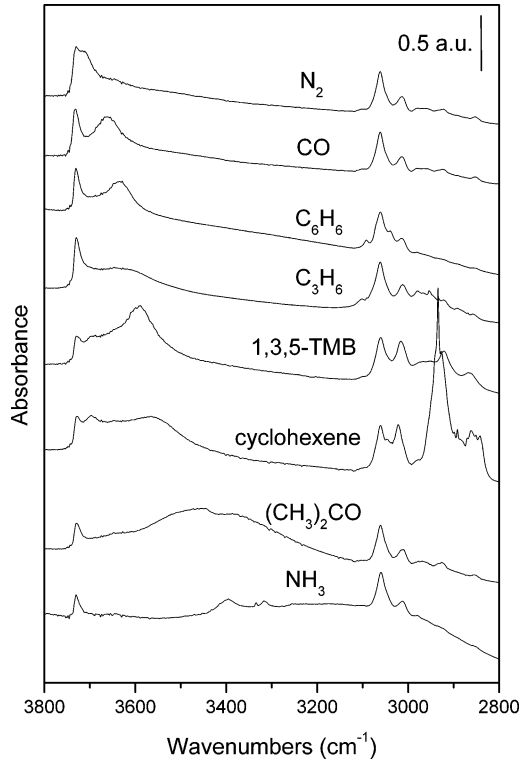

Figure 4. IR spectra illustrating the adsorption of different probe molecules: proton affinity of the probe increases downward.

TABLE 3: Experimental OH Frequency Shifts ($\Delta\nu$(OH), cm^{-1}) Observed for Isolated Silanol in Amorphous Silica and Benzene−Silica

probe	SiO_2	benzene−silica
N_2	40	27
CO	90	73
C_6H_6	120	97
C_3H_6	152	125
1,3,5-TMB	167	139
cyclohexene	173	144
methylacetylene	210	174
acetone	345	312
NH_3	650	630

that the two sets of data yield a straight line, passing through the origin, with a slope about 0.93.

The conclusion is that the presence of a phenyl group, with respect to silica, induces a lesser acidity. The same conclusion is afforded by the computational results.

Figure 6 illustrates the structure of the adducts between SILH and a few probe molecules: CO, ammonia, and formaldehyde (considered instead of the more complex acetone molecule used in experiments), as compared to similar adducts formed with SIL. Corresponding BE values are reported in Table 4: the strength of interaction is in the order CO, aldehyde, and ammonia with both acidic species, and SILH is seen to be less acidic than SIL, because slightly lesser values are observed. The intermolecular distance between the acidic proton in either SIL or SILH and the basic atom in the molecule (C, O, and N, respectively) scales with the strength of interaction, both as it concerns the sequence in basic molecules and the comparison between SIL and SILH.

The calculated values for the shift in OH stretch are reported in Table 4; with the slight exception of CO, basically yielding the same value, shifts in the OH stretching modes confirm the lesser acidity of SILH with respect to SIL.

Thermodynamics of Interaction. Being both with silica and benzene−silica that all interactions are weak and reversible, it

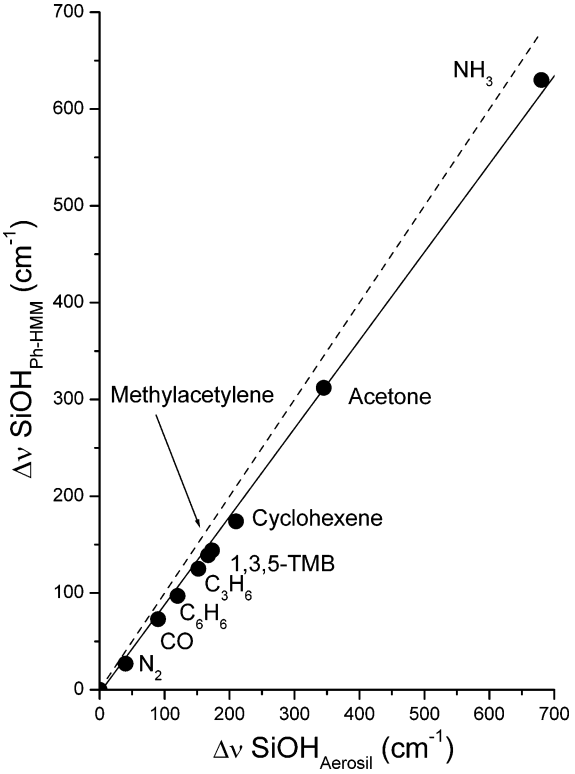

Figure 5. Bellamy−William−Hallam plot comparing the shifts observed with pure amorphous silica (Aerosil, literature data) and those observed with benzene−silica (this work). The broken line is the bisectrix with unit slope.

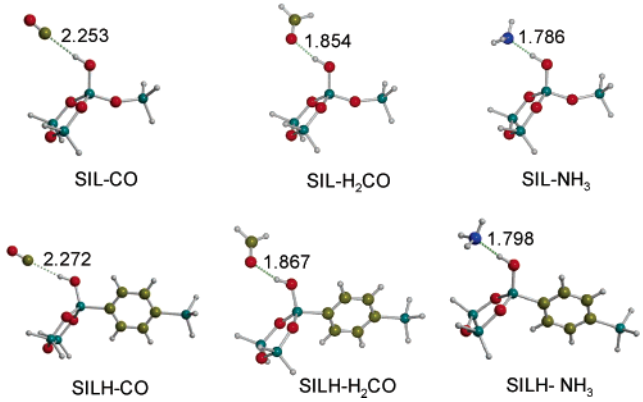

Figure 6. B3LYP/6-31+G(d,p) optimized structures of intermolecular complexes between SIL (or SILH) and CO, H_2CO, and NH_3, respectively. Intermolecular bond length in Å.

TABLE 4: B3LYP/6-31+G(d,p) Binding Energy (BE, kJ/mol) and OH Harmonic Frequency Shifts ($\Delta\omega_h$(OH), cm^{-1}) of SIL and SILH Interacting with CO, H_2CO, and NH_3 Molecules

system	BE	$\Delta\omega_h$(OH)[a]
SIL−CO	4.8	−83
SIL−H_2CO	25.7	−260
SIL−NH_3	44.3	−626
SILH−CO	4.3	−84
SILH−H_2CO	25	−251
SILH−NH_3	43	−597

[a] $\Delta\omega_h$(OH) = ω_h (OH-complex) − ω_h (OH-free model).

is possible, given a certain molecule, to take spectra at increasing equilibrium pressure p and to measure the decreasing intensity A of the silanols stretching band. The fraction of silanols θ engaged in H-bonding is readily calculated as (A°−A)/A°,

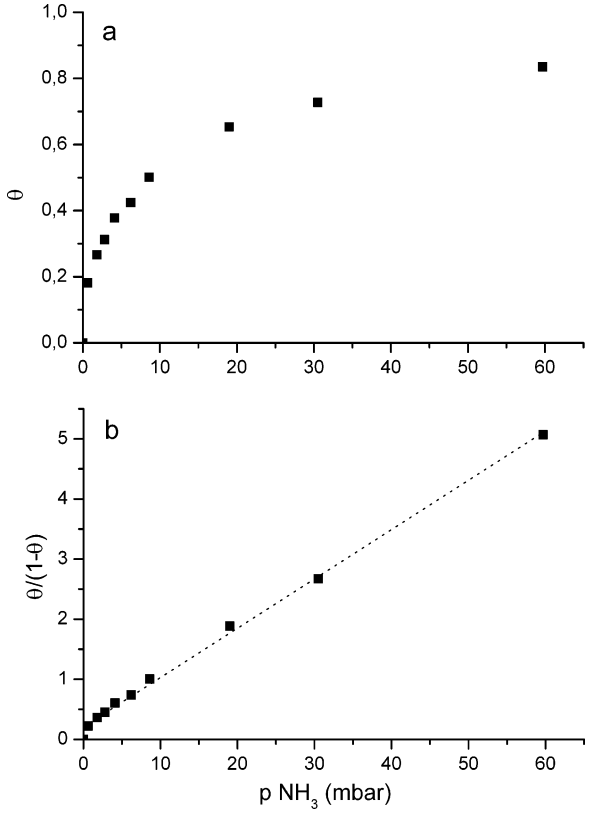

Figure 7. (a) Optical adsorption isotherms for ammonia on benzene−silica outgassed at 450 °C. (b) Linearized form of the Langmuir isotherm.

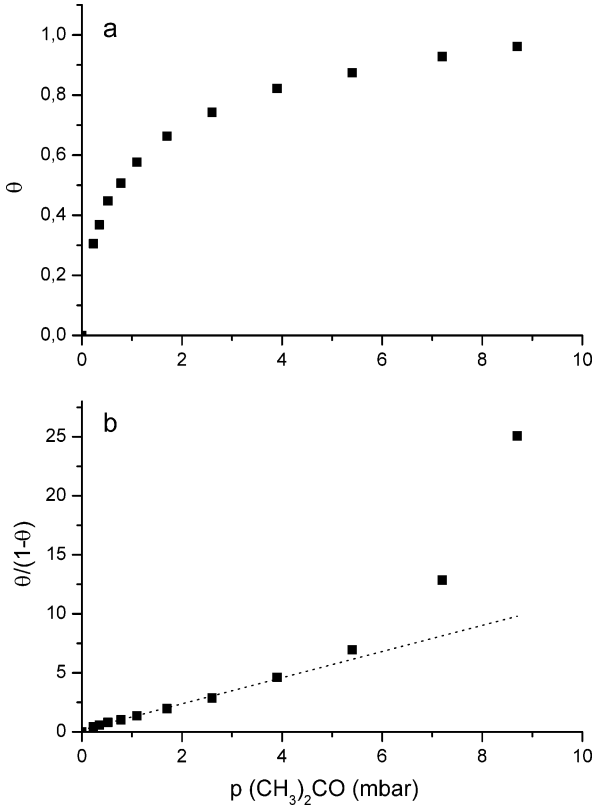

Figure 8. (a) Optical adsorption isotherms for acetone on benzene−silica outgassed at 450 °C. (b) Linearized form of the Langmuir isotherm.

$A°$ being the intensity of the silanol peak of the naked sample. This procedure allows the quantitative description of the H-bond interaction. This resembles an adsorption isotherm and, because it is obtained via optical measure, it will be referred to in the following as optical isotherm.[26]

Figure 7a reports such optical isotherms for NH_3 and acetone on benzene−silica: results for mesoporous silica are similar and are not reported. The curve for ammonia follows strictly the Langmuir formula $\theta = Kp/(1 + Kp)$: section b of the figure shows that the quantity $\theta/(1-\theta)$ is indeed proportional to the pressure, the proportionality factor being the equilibrium constant of the process Si−OH + M(g) ↔ SiOH···M. The values of K are 8 10^{-2} ($mbar^{-1}$) for silica and 7 10^{-2} ($mbar^{-1}$) for benzene−silica; the small difference, if meaningful, is ascribable to the lesser acidity of SiOH in the latter system.

The case of acetone is more complex because solvation of H-bonded molecules by other surrounding molecules takes places at high pressures: the Langmuir behavior is not observed over the entire range, but the linear portion of the corresponding plot in section b allows, however, to calculate the equilibrium constants. That for the benzene−silica results is 0.95 $mbar^{-1}$, definitely larger than that for mesoporous silica (0.31 $mbar^{-1}$), notwithstanding the lesser acidity of the former. This is probably evidence that secondary interactions take place. Besides the main interaction (H-bonding between the C═O group and the silanol), H-bonding via the slightly acidic C−H groups of acetone may occur with neighboring aromatic rings, as well as dispersive interactions with the same aromatic rings.

This finding suggests a role of the aromatic portion of the surface in the adsorption and interaction with guest molecules, confirming the bifunctional nature of the surface.

Conclusions

Hydroxyl species of mesoporous benzene−silica hybrid material with crystal-like wall structure outgassed at 723 K mainly consist of noninteracting isolated silanols, showing both the O−H and Si−O stretching modes at lower frequencies than those well-known for SiOH species in amorphous silica. Both experimental and computational evidence indicate that the aryl group in the coordination sphere of Si induces a lesser acidity with respect again to the isolated silanol in silica. This notwithstanding, optical isotherms show that the interaction with acetone is stronger with benzene−silica than with silica: this is interpreted in terms of secondary interactions between the slightly acidic CH in acetone and the electronic cloud in benzene-like rings. This suggests that both the inorganic component and the organic one play a role in dictating the surface behavior.

Acknowledgment. The authors acknowledge financial support from MIUR (Ministero Italiano dell'Università e della Ricerca), ASI (Agenzia Spaziale Italiana, progetto ZEUS), and JST (Japan Science and Technology Agency) and computational support from CINECA supercomputing center.

References and Notes

(1) Yoshina-Ishii, C.; Asefa, T.; Coombs, N.; MacLachlan, M. J.; Ozin, G. A. *Chem. Commun*. **1999**, 2539.

(2) Inagaki, S.; Guan, S.; Fukushima, Y.; Ohsuna, T.; Terasaki, O. *J. Am. Chem. Soc.* **1999**, *121*, 9611.

(3) Lu, Y.; Fan, H.; Doke, N.; Loy, A. D.; Assink, R. A.; LaVan, D. A.; Brinker, C. J. A. *J. Am. Chem. Soc*. **2000**, *122*, 5258.

(4) Goto, Y.; Inagaki, S. *Chem. Commun*. **2002**, 2410.

(5) Kuroki, M.; Asefa, T.; Whitnal, W.; Kruk, M.; Yoshina-Ishii, C.; Jaroniec, M.; Ozin, G. A. *J. Am. Chem. Soc.* **2002**, *124*, 13886.

(6) Bion, N.; Ferreira, P.; Valente, A.; Gonçalves, I. S.; Rocha, J. *Chem. Commun*. **2003**, 1910; Wang, W.; Zhou, W.; Sayari, A. *Chem. Mater*. **2003**, *15*, 4886.

(7) Yang, Q.; Kapoor, M. P.; Inagaki, S. *J. Am. Chem. Soc*. **2002**, *124*, 9694.

(8) Inagaki, S.; Guan, S.; Ohsuna, T.; Terasaki, O. *Nature* **2002**, *416*, 304.

(9) Frisch, M. J.; Trucks, G. W.; Schlegel, H. B.; Scuseria, G. E.; Robb, M. A.; Cheeseman, J. R.; Zakrzewski, V. G.; Montgomery, J. A., Jr.; Stratmann, R. E.; Burant, J. C.; Dapprich, S.; Millam, J. M.; Daniels, A. D.; Kudin, K. N.; Strain, M. C.; Farkas, O.; Tomasi, J.; Barone, V.; Cossi, M.; Cammi, R.; Mennucci, B.; Pomelli, C.; Adamo, C.; Clifford, S.; Ochterski, J.; Petersson, G. A.; Ayala, P. Y.; Cui, Q.; Morokuma, K.; Malick, D. K.; Rabuck, A. D.; Raghavachari, K.; Foresman, J. B.; Cioslowski, J.; Ortiz, J. V.; Stefanov, B. B.; Liu, G.; Liashenko, A.; Piskorz, P.; Komaromi, I.; Gomperts, R.; Martin, R. L.; Fox, D. J.; Keith, T.; Al-Laham, M. A.; Peng, C. Y.; Nanayakkara, A.; Gonzalez, C.; Challacombe, M.; Gill, P. M. W.; Johnson, B. G.; Chen, W.; Wong, M. W.; Andres, J. L.; Head-Gordon, M.; Replogle, E. S.; Pople, J. A. *Gaussian 98*, revision A.7; Gaussian, Inc.: Pittsburgh, PA, 1998.

(10) Becke, A. D. *J. Chem. Phys.* **1993**, *98*, 5648.

(11) Lee. C.; Yang, W.; Parr, R. G. *Phys. Rev. B* **1988**, *37*, 785.

(12) Civalleri, B.; Garrone, E.; Ugliengo, P. *J. Phys. Chem. B* **1998**, *102*, 2373.

(13) Lindberg, B. *J. Chem. Phys.* **1988**, *88*, 380.

(14) Ugliengo, P. ANHARM − *A program to solve monodimensional nuclear Schrodinger equation*; Università di Torino, Torino, Italy, 1989, unpublished.

(15) Ugliengo, P.; Viterbo, D.; Borzani, G. *J. Appl. Cryst.* **1988**, *21*, 75.

(16) Ugliengo, P.; Viterbo, D.; Chiari, G. *Z. Kristallogr*. **1993**, *9*, 207.

(17) Ryason, P. R.; Russell, B. G. *J. Phys. Chem*. **1975**, *79*, 1276. Boccuzzi, F.; Coluccia, S.; Ghiotti, G.; Morterra, C.; Zecchina, A. *J. Phys. Chem*. **1978**, *82*, 1298.

(18) Civalleri, B.; Garrone, E.; Ugliengo, P. *Chem. Phys. Lett*. **1998**, *294*, 103.

(19) Shimanouchi, T. Molecular Vibrational Frequencies. In *NIST Chemistry WebBook*, NIST Standard Reference Database Number 69; Linstrom, P. J., Mallard, W. G., Eds.; National Institute of Standards and Technology: Gaithersburg, MD, 2003; (http://webbook.nist.gov).

(20) Kuroki, M.; Asefa, T.; Whitnal, W.; Kruk, M.; Yoshina-Ishii, C.; Jaroniec, M.; Ozin, G. A. *J. Am. Chem. Soc*. **2002**, *124*, 13886.

(21) Asefa, T.; Maclachlan, M. J.; Grondey, H.; Coombs, N.; Ozin, G. A. *Angew. Chem., Int. Ed*. **2000**, *39*, 1808.

(22) Siesler, H. W. *Infrared and Raman Spectroscopy of Polymers*; Marcel Dekker: New York, 1980.

(23) Ou, L. D.; Seddon, A. B. *J. Non-Cryst. Solids* **1997**, *210*, 187.

(24) Rouxhet, P. G.; Sempels, R. E. *J. Chem. Soc., Faraday Trans. 1* **1974**, *70*, 2021.

(25) Curthoys, G.; Davydov, V. Ya.; Kiselev, A. V.; Kiselev, S. A.; Kuznetsov, B. V. *J. Colloid Interface Sci.* **1974**, *48*, 58.

(26) Onida, B.; Allian, M.; Borello, E.; Ugliengo, P.; Garrone, E. *Langmuir* **1997**, *13*, 5107. (b) Garrone, E.; Barbaglia, A.; Onida, B.; Civalleri, B.; Ugliengo, P. *Phys. Chem. Chem. Phys*. **1999**, *1*, 4649.